Manuscript for Annual Meeting Compendium of Papers

Lateral Force Measurement in Concrete Crosstie Fastening Systems

TRB 14-3112

Transportation Research Board 93rd Annual Meeting

Submitted: 1 August 2013

Brent A. Williams[1,2], Ryan G. Kernes[2], J. Riley Edwards[2], and Christopher P. L. Barkan[2]

Rail Transportation and Engineering Center – RailTEC
Department of Civil and Environmental Engineering
University of Illinois at Urbana-Champaign
205 N. Mathews Ave., Urbana, IL 61801

4,608 Words, 8 Figures, 1 Table = 6,858 Total Word Count

Brent A. Williams
(603) 562-5515
bwillms3@illinois.edu

Ryan G. Kernes
(217) 333-6232
rkernes2@illinois.edu

J. Riley Edwards
(217) 244-7417
jedward2@illinois.edu

Christopher P. L. Barkan
(217) 244-6338
cbarkan@illinois.edu

[1]Corresponding author

ABSTRACT

A steady increase in cumulative freight tonnages, as well as growing high-speed intercity passenger rail operation, has placed greater demands on North American railroad infrastructure. The insulator in concrete crosstie fastening systems is a key component that is known to fail in demanding loading environments. This failure can cause track geometry defects and frequent maintenance procedures that decrease track capacity and increase operating costs. A failed insulator occurs when the component is unable to perform its design function due to abrasion, fracturing, or crushing caused by excessive movement or forces in the fastening system. Lateral forces transferred through the fastening system are thought to be a primary contributor to the degradation of insulators. A lack of understanding of these lateral forces has led to an iterative design process for the insulator and the concrete crosstie and fastening system. The objective of this study is to understand, map, and quantify the lateral load path by measuring the magnitude of lateral forces entering the shoulder, a component of the fastening system adjacent to the insulator. To measure these forces, the Lateral Load Evaluation Device (LLED) was developed at UIUC. The data captured by the LLED will assist the rail industry in mechanistically designing future fastening systems by understanding the magnitude, distribution, and path of lateral forces in the fastening system. Information gained by the LLED will also lead to a greater understanding of the frictional forces at key interfaces in the fastening system. Preliminary results show that the magnitude, distribution, and path of lateral forces vary considerably between adjacent crossties and depend heavily on the lateral stiffness of the fastening system.

INTRODUCTION

Concrete crossties are typically installed in demanding operating conditions, such as locations with heavy axle load freight traffic, steep grades, high degrees of curvature, severe climates, high speed rail traffic, or other passenger rail traffic that requires stringent geometric tolerances. These operating environments may be too harsh for conventional timber crossties, limiting crosstie life cycles. Even though concrete crossties may provide a better option than conventional timber crossties in severe conditions, they are not without their design and performance challenges. A recurring problem in concrete crosstie fastening systems involves the component known as the insulator, which is located between the top of the rail base and the anchorage point for the elastic clip known as the shoulder. Most frequently, the insulator post, the section of the insulator between the side of the rail base and cast-in shoulder, is the most common location of damage on insulators. Final results from surveys of North American Class I Railroads conducted in 2008 and 2012 showed that shoulder/fastener wear or fatigue was the second most critical concrete crosstie problem (*1*). The increased number of component interactions due to the insulator contacting most components in the fastening system makes it a critical component in concrete crossties and its failure can be related to a number of concrete crosstie problems (*2)*.

Insulators are designed as sacrificial wear components within the fastening system so that they wear as opposed to the rail or shoulder. However, insulator failure occurs when the geometry and strength of the component is degraded such that it can no longer meet its function and designed performance characteristics, which include providing gauge restraint, attenuating the forces entering the shoulder, providing electrical isolation, and transmitting clamping force from the clip to the rail. When an insulator failure occurs, some track geometry defects (e.g. wide gauge) become more prevalent. Worn or missing insulators can facilitate excessive rail movement, further expediting failure of other fastening system components or the concrete crosstie itself. Additionally, insulator post wear may have a direct influence on the rate of rail seat abrasion and premature rail pad failure (*3)*. Insulator failures were first seen by North American railroads in the spring of 1988, just nine months after their installation. Since that time, the life of rail has increased at a rate that exceeds that of the fastening system components, leading to maintenance activities that are focused solely on the fastening system. Although rail life has increased due to design alterations and better material selection, a fastening system has yet to be developed to match the life of the rail in demanding service environments.

Due to the lack of prior research in the area of insulator failure, a simplified Failure Mode and Effect Analysis (FMEA) was used to guide our approach to addressing this problem. The FMEA was used to define and identify the modes of failure, their causes, and the effects they have on other fastening system components and the system as a whole (4). The outcome of the FMEA narrowed our focus to three primary causes of insulator failure: abrasion, fracturing, or crushing. Abrasion occurs when relative motion occurs between the insulator and the iron shoulder or rail base. This relative motion, combined with fines such as sand particles, will ultimately degrade the insulator causing track geometry defects. Fracturing of the insulator will occur when forces are applied in a way that causes the component to fracture or crack due to brittleness. The same track geometry defects can be seen when the component fractures and cannot provide the necessary restraint or insulation. Lastly, crushing occurs when the lateral force the insulator post is subjected to exceeds the strength of the material. It should also be noted that environmental conditions, such as ultraviolet (UV) light or moisture exposure, can alter material properties and initiate failure (*5*).

By quantifying the lateral forces passing through the insulator, we gain valuable insight into the demands placed on it, allowing for mechanistic design. Mechanistic design is a process derived from analytical and scientific principles, considering field loading conditions and performance requirements. (*6*). To better understand the forces acting on the insulator and how they are distributed, researchers at the University of Illinois at Urbana-Champaign (UIUC) have designed the Lateral Load Evaluation Device (LLED) to measure the lateral force passing through the insulator post and entering the shoulder face. Previous attempts to measure this force have been unsuccessful for a variety of reasons. UIUC researchers have devised a novel approach, which has allowed us to successfully measure the lateral force in both laboratory and field settings.

BACKGROUND

Thus far, lateral forces in concrete crosstie fastening systems have not been quantified or understood at a level that would guide design and maintenance practices. UIUC and other researchers have succeeded in measuring and quantifying the load path in the vertical direction through the use of strain gauges in the crib of rail and additional instrumentation in the fastening system (*7*). As a part of quantifying the vertical load path, researchers at UIUC have successfully implemented matrix based tactile surface sensors (MBTSS) to measure the forces and pressure distribution in the vertical direction at the interface of the rail pad and concrete rail seat (*8*). However, there have been limited attempts to quantify the lateral load path through the fastening system (*9*).

Many factors affect the lateral forces at the insulator-shoulder interface. The magnitude of lateral load is a function of the lateral to vertical (L/V) load ratio and is highly dependent on the geometry of the track (e.g. horizontal curves). Curves can generate considerable lateral loads on both the high rail and low rail depending on the speed of the train and the amount of superelevation of the curve. Lateral forces and train performance in curves are both engineering and operational concerns on shared freight and passenger infrastructure due to the fact that speeds can vary significantly. Additionally, the presence of top-of-rail (TOR) friction modifiers or moisture on the surface of the rail can affect the L/V ratio and the resulting magnitude of lateral forces (*10)*. Also, it is desirable for both cant and degree of curvature to be as uniform as possible throughout the body of the curve, to avoid undesirable lateral shocks on the vehicle. Irregularities in track gauge and alignment on both tangent and curved track cause vehicle oscillation and result in higher lateral forces (*11*). Ultimately, the design and performance of the fastening system governs the transfer of these lateral loads into the crosstie. Given the numerous factors that can impact the magnitude of lateral loads, the design of the fastening system for lateral load attenuation is a critical topic that deserves further research. This paper presents results from field experiments that were designed to understand the variables that affect the magnitude and distribution of lateral forces in the fastening system, particularly those forces passing through the insulator post and entering the shoulder.

MEASUREMENT TECHNOLOGY

Researchers at UIUC developed a technology to measure the lateral force at the insulator-shoulder interface while maintaining the original geometry of a concrete crosstie Safelok I fastening system. This approach was developed after learning from earlier attempts aimed at measuring the lateral force passing through the insulator post and entering the shoulder. UIUC's Lateral Load Evaluation Device (LLED) uses strain gauges to measure bending strain of a four-point-contact beam. The face of the shoulder is grinded away using a handheld grinder and straight edge to ensure proper dimensions are maintained. Once the shoulder face is removed, the LLED replaces it. Figure 1 illiustrates how the lateral force passing through the insulator post is transferred to the beam, inducing bending. Figure 2 shows an LLED installed before the clip is driven on the system. The primary advantage of this technology is that the orignal geometry is maintained, thus clip installation procedures and all fastening system components remain the same. The

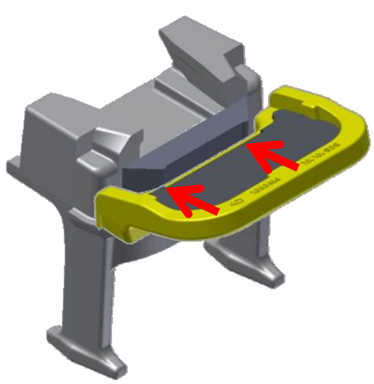

Figure 1 Lateral load transfer into LLED

Figure 2 LLED installed on shoulder

LLED also provides valuable insight into where lateral forces are transferred in the fasteing system. Frictional forces at the rail-rail pad and insulator-clip toe interfaces also resist lateral load and are assumed to be the difference between the input load and LLED measurement. Additionally, lateral rail flexure may resist some small amounts of force, but the resistance is assumed to be negligible based on theoretical calculations that are in agreement with the response of a validated finite element (FE) multi-tie model that is available at UIUC (*12*). Because lateral restraint is primarily a function of the fasteing system, this research will allow us to understand how variables associated with friction (e.g. materials and geometry) alter the lateral load path (*13*). Therefore, data obtained by the LLED will aid future fastening system design by quantifying the lateral loads.

Each LLED beam has two defined points of contact with the shoulder that act as outer supports and two defined points of contact with the insulator that are narrower than the supports. Together, this geometry induces a bending action of the beam under load. The beam contains four strain gauges which are wired into a full Wheatstone Bridge to measure bending strain under load. These strains are subsequently resolved into a force using calibration curves generated prior to testing using a uniaxial loading frame. For calibration, LLEDs were supported on a level plate by two small steel blocks and loaded with a self-leveling loading head to ensure perpendicular loading. Furthermore, frictional forces between the bottom of the LLED and the ground shoulder are assummed to be negligible because there was no vertical normal force applied to the LLEDs. In laboratory and field installations a thin steel insert (20 gauge/0.0359 inches/0.9119 mm) was used between the insulator and the two points of contact on the beam to ensure the points of loading would not penetrate into the relatively soft insulator material (Nylon 6/6) turning the two-point load into a distributed load, and negatively impacting the accuracy of the results (*6)*. The end result is a load cell at the shoulder-insulator interface that leaves original geometry and loading conditions of the shoulder and insulator unaffected.

EXPERIMENTAL SETUP

Field experimentation was conducted at the Transportation Technology Center (TTC) in Pueblo, Colorado. Field experiments and results described in this paper were conducted on a segment of tangent track on the Railroad Test Track (RTT) at TTC. Although curved sections of track are likely to experience higher lateral forces than tangent sections, the RTT was chosen to understand how tangent track (with concrete crossties and an elastic fastening system) distributes the lateral forces without geometry-induced variability associated with curvature. Different static loading scenarios (e.g. magnitudes, L/V ratios, etc.) were applied to each section of track using the Track Loading Vehicle (TLV). The TLV uses a single deployable split-axle with a wheelset capable of applying various combinations of vertical and lateral loads simultaneously to both rails to represent loading conditions of a railcar wheel. The test section used a 136RE rail section,

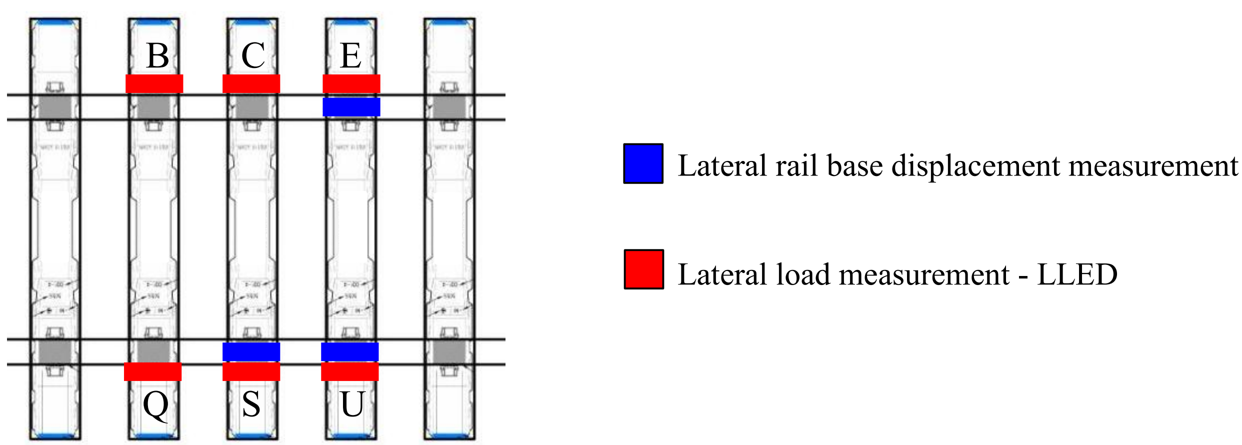

Figure 3 Instrumentation Locations

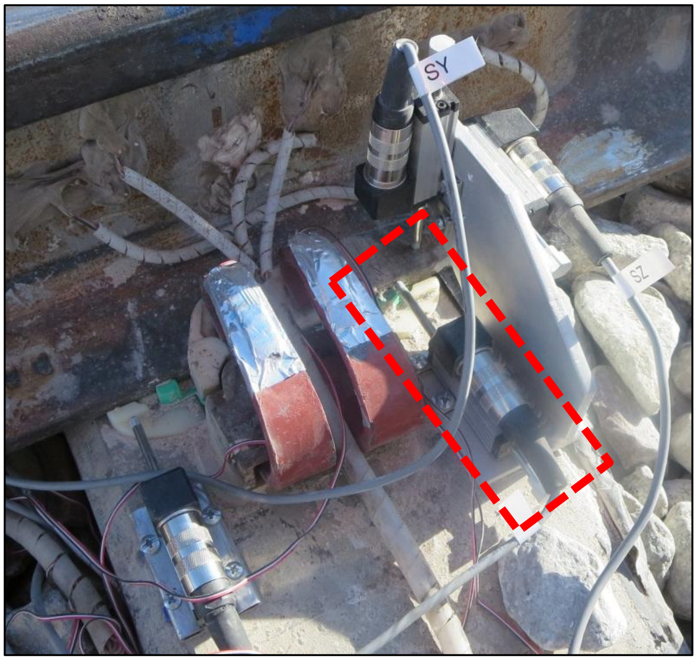

Figure 4 Field setup to measure lateral rail base displacement

concrete crossties spaced at 24 inches (610 mm) center-to-center, and premium ballast with an average of 16 inches (406 mm) of shoulder ballast. New fastening system components were used during testing, in an effort to ensure the uniformity of the fastening system components. LLEDs deployed at TTC were installed on the field side of the rail on both rail seats of three adjacent concrete crossties. The field side was chosen due to the vast majority of insulator failures being seen on the field side. Figure 3 shows the location and naming convention of LLEDs. The installation first required removing the clips and rail pad assembly from the rail seat. Next, the shoulder face was grinded away, and new rail pad assemblies, insulators, and clips were installed. The LLED was then installed in place of the shoulder face.

Lateral rail base displacements were also measured in conjunction with the LLEDs. A potentiometer was fixed perpendicular to the rail on the crosstie and contacted the rail base (Figure 4). This displacement, when compared with the lateral force measured at the corresponding shoulder face, describes the lateral stiffness of the fastening system. Lateral stiffness measurements were captured at three of the six LLED locations, since they overlapped with lateral rail base displacement measurements. In this paper, the term lateral stiffness refers to the change in rail base displacement for a given change in lateral force in the shoulder as measured in the field.

EXPERIMENTATAL RESULTS

The test matrix for TLV loading on the RTT included many unique loading scenarios (e.g. varying L/V ratios, load magnitudes, etc.). However, for the purpose of this paper, a 40 kip (178 kN) vertical load and varying lateral loading scenario resulting in a maximum 0.55 L/V force ratio will be discussed, to provide a means of comparison between the rail seats. Additionally, we will focus on load application at two discrete locations on the test section: crosstie E-U and crosstie C-S (Figure 3).

When a 20 kip (89 kN) lateral load was applied at crosstie E-U, the measured lateral forces at the insulator-shoulder interface on rail seat E and U were 5,520 lbs (25 kN) and 3,782 lbs (17 kN), respectively (Figure 5). Likewise, the measured lateral forces at the insulator-shoulder interface on rail seat C and S were 4,315 lbs (19 kN) and 3,420 lbs (15 kN), respectively (Figure 5). While the difference between lateral force measured at adjacent rail seats E and C is 1,205 lbs (6 kN), the difference between adjacent rail seats U and S is only 362 lbs (2 kN). This indicated an even distribution of lateral forces between adjacent rail seats, contrary to conventional engineering intuition that the support (i.e. rail seat) directly beneath the

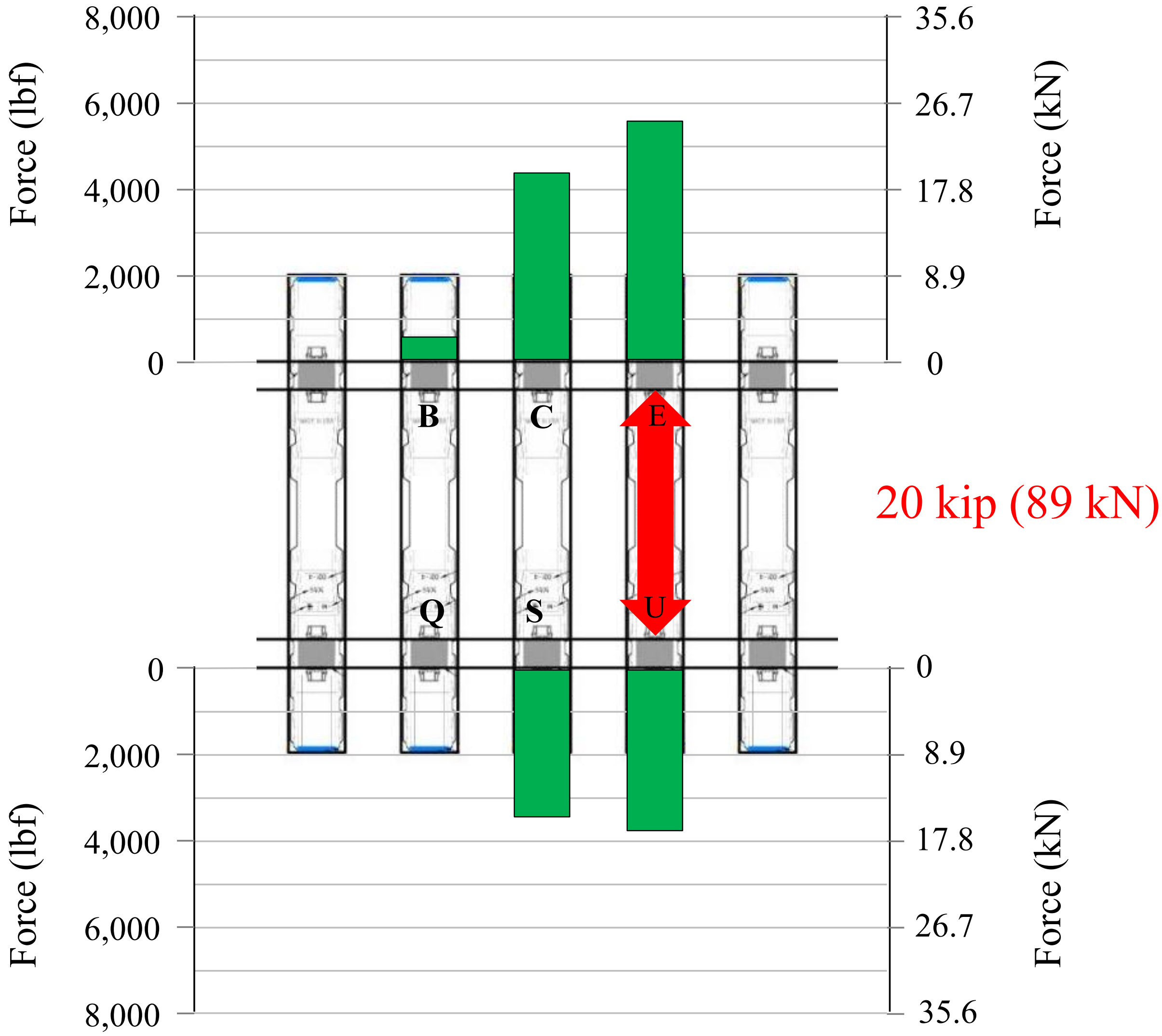

Figure 5 Lateral Forces due to Loading at Crosstie E-U

applied load would carry the most load. However, when the loading location is moved to crosstie C-S and an equivalent load is applied, the distribution of lateral forces changes dramatically from what is seen when loaded at crosstie E-U.

When a 20 kip (89 kN) lateral load was applied at crosstie C-S, the measured lateral forces at the insulator-shoulder interface on rail seat C and S were 6,380 lbs (28.4 kN) and 6,980 lbs (31 kN), respectively (Figure 6). Likewise, the measured lateral forces at the insulator-shoulder interface on rail seat E and U were 1,325 lbs (5.9 kN) and 540 lbs (2.4 kN), respectively (Figure 6). The difference between lateral forces measured at adjacent rail seats C and E and adjacent rail seats S and U are much higher when loaded at crosstie C-S than when loaded at crosstie E-U. The difference between lateral force measured at adjacent rail seats C and E is 5,055 lbs (22.5 kN), while the difference between adjacent rail seats U and S is 6,440 lbs (28.6 kN). This distribution of lateral forces when loaded at crosstie C-S is significantly different than the distribution when loaded at crosstie E-U. To better understand why this variance of lateral force distribution exists, the lateral stiffness of adjacent rail seats S and U was investigated.

Lateral displacements of the rail base were taken at rail seats S and U to understand the lateral translation of the rail. This measurement was used in conjunction with the LLED at the corresponding rail seat to generate force-displacement curves, ultimatelv allowing for quantification of the lateral stiffness of

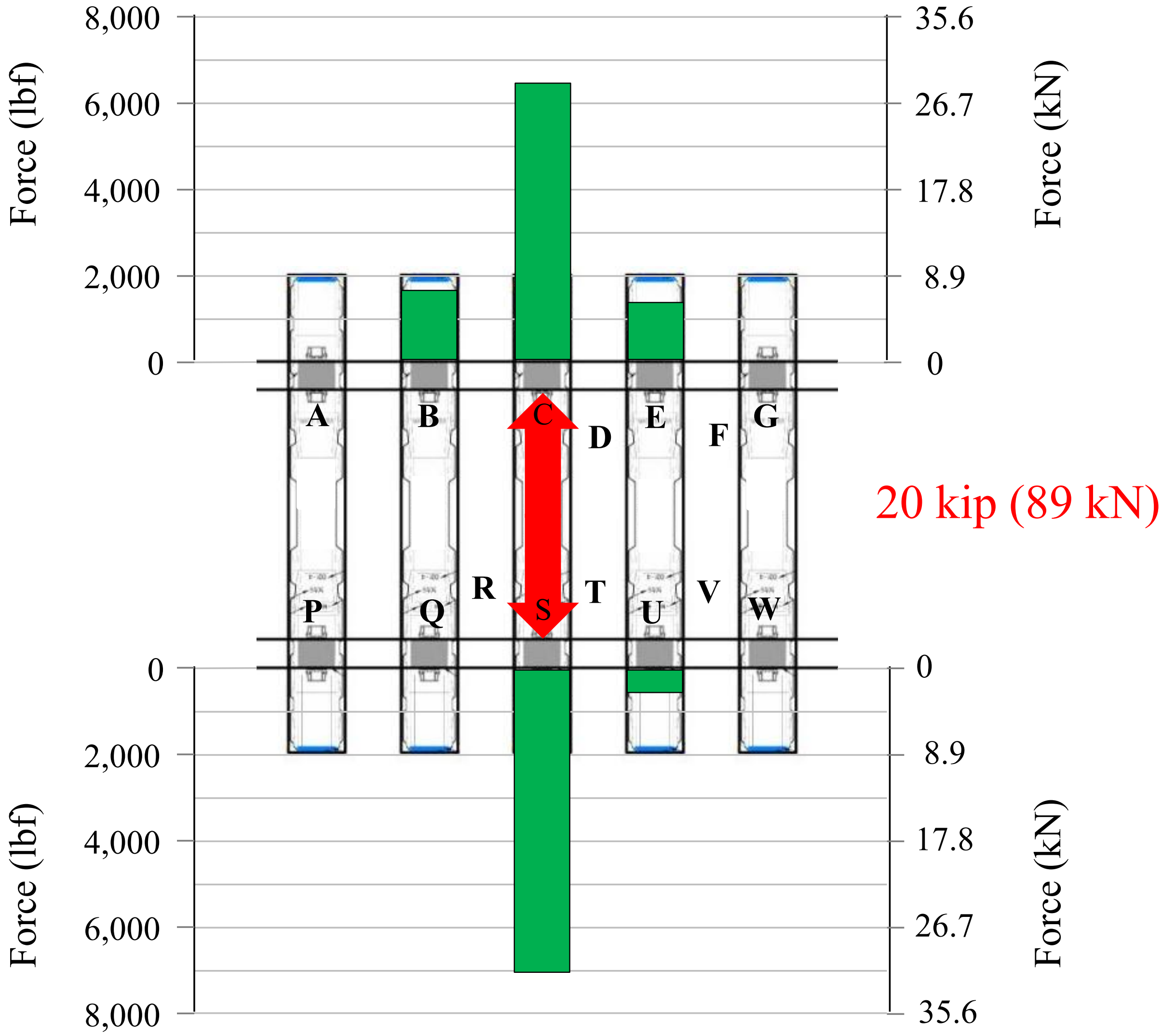

Figure 6 Lateral Forces due to Loading at Crosstie C-S

the fastening system at the insulator-shoulder interface. When load was applied at crosstie E-U, rail seat U has a lateral stiffness of 146,322 lbs/in (25.6 kN/mm) (Figure 7). In comparison, when load was applied at crosstie C-S rail seat S has a lateral stiffness of 192,498 lbs/in (33.7 kN/mm) (Figure 7), which is 32% stiffer than rail seat U. Referring to the load magnitude data, when load was applied at crosstie E-U, rail seat U shared roughly equal magnitudes of lateral force with adjacent rail seat S. However, when the loading location was moved to crosstie C-S, rail seat S carried about 6,500 lbs (29.8 kN) more than adjacent rail seat U. This indicates that rail seat S carries more lateral force than rail seat U due to increased lateral stiffness.

The magnitude of lateral force measured at rail seat S when loaded at crosstie C-S was 104% more than the lateral force measured at rail seat U when loaded at crosstie E-U. This indicates that a lateral stiffness increase of about 30% can increase the lateral load carried by a rail seat by more than 100% (i.e. a factor of two).

The lateral stiffness and magnitude data obtained from rail seats S and U provide a proxy for understanding how lateral loads are transferred in a fastening system in one of two ways. Because the measured lateral forces increased significantly with increasing lateral stiffness, larger lateral forces at a particular rail seat may indicate that the rail seat has a higher lateral stiffness. The lateral stiffness of the fastening system is a function of fastener design parameters (e.g. pad material properties, clamping force) and can affect the lateral forces at the insulator-shoulder interface. However, variances in stiffness among adjacent rail seats are likely to occur in the field due to factors associated with installation procedures, such as gaps between fastening system components. Also, shoulder position tolerances (e.g. relative position to one another on crosstie as well as crosstie-to-crosstie) could have altered the stiffnesses at each rail seat. Since the fastening system was held constant for this experiment, factors due to installation and shoulder position variability were the likely causes of variation. Figure 8 shows the maximum lateral forces measured by LLEDs at each rail seat under a 22 kip (98 kN) lateral load and a 0.5 L/V ratio. Given rail seat S and U had a lateral stiffness of 192,498 lbs/in (33.7 kN/mm) and 146,322 lbs/in (25.6 kN/mm), respectively, rail seat E should have a lateral stiffness between those two values due to the fact that the measured lateral force at rail seat E was 5,585 lbs (25 kN). The lateral stiffness at rail seat E was 155,369 lbs/in (27.2 kN/mm) (Figure 7), 6% higher than the lateral stiffness at rail seat U. The 5,585 lbs (25 kN) measured at rail seat E is also 20% higher than the 4,635 lbs (20.6 kN) measured at rail seat U, showing us that relatively small increase in lateral stiffness will ultimately result in a larger increase in load carried. To further validate this hypothesis, the data show that lateral stiffness at rail seat S is 24% higher than the lateral stiffness at rail seat E, while the maximum lateral force measured at rail seat S is 40% higher than rail seat E.

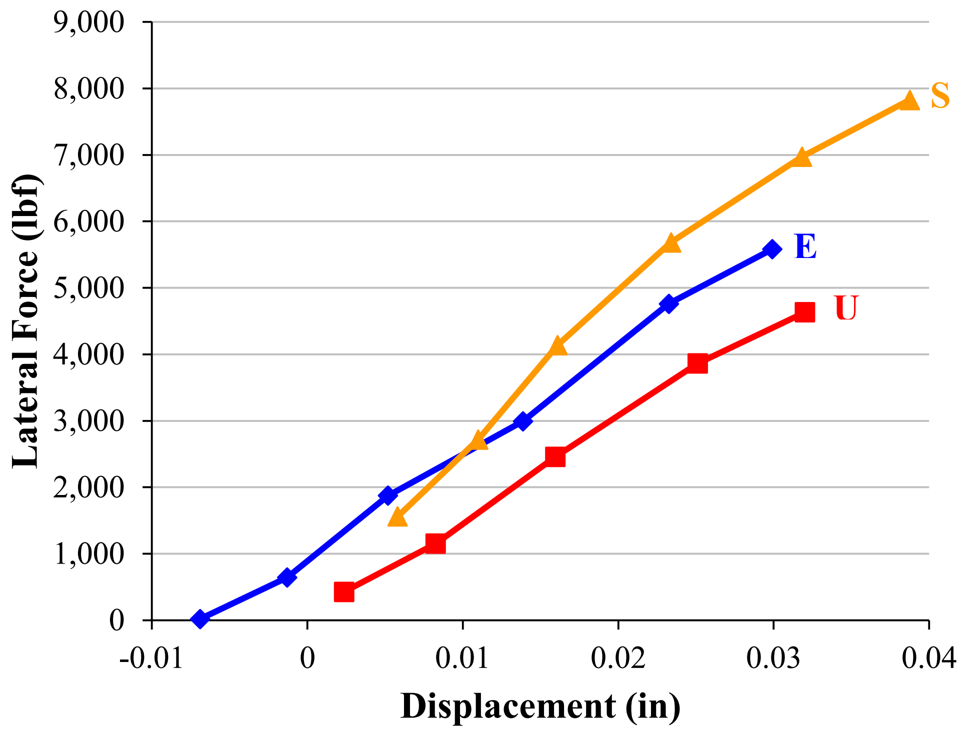

Figure 7 Lateral Stiffness at Rail Seats S, E, and U

Table 1 Linear Trendline Data for Lateral Stiffness of Rail Seats S, E, and U

Rail Seat	Equation of Linear Trendline	R^2 Value	Lateral Stiffness (lbf/in)
S	y = 192,498x + 747.32	0.98	192,498
E	y = 155,369x + 988.07	1.00	155,369
U	y = 146,322x + 57.37	1.00	146,322

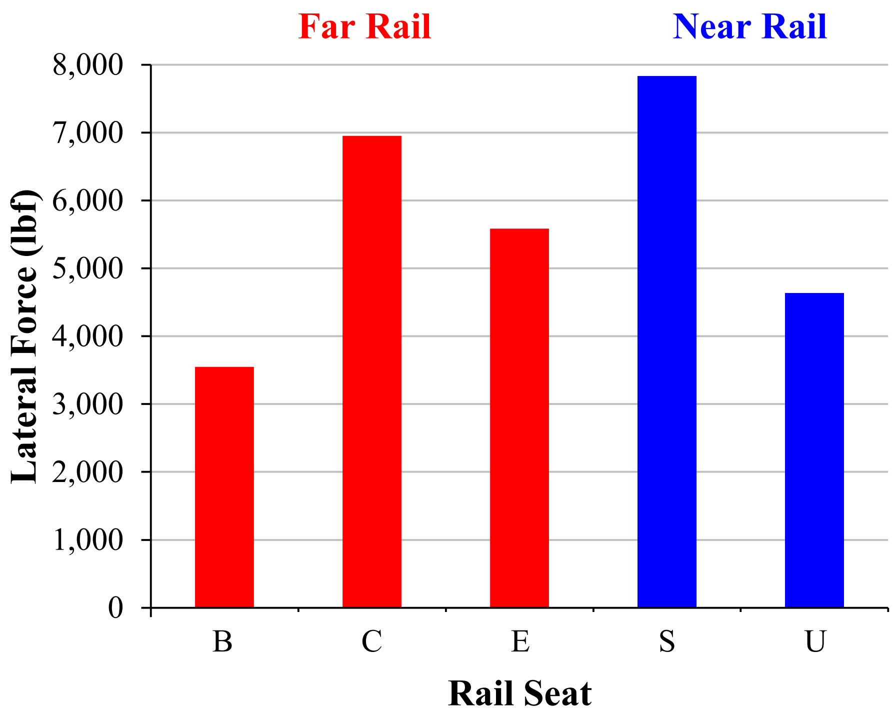

Figure 8 Maximum Lateral Force When a 22 kip (98 kN) Load is Applied Directly Over the Referenced Rail Seat

CONCLUSIONS

The Lateral Load Evaluation Device (LLED) developed at UIUC has proven to be a successful instrumentation technology to quantify lateral loads at the shoulder face-insulator interface. Field observations show a high degree of correlation with the data obtained from laboratory testing and result in the following preliminary conclusions:

- As hypothesized, under our experimental conditions, a rail seat with a higher lateral stiffness results in a higher percentage of lateral load bearing on the insulator post and shoulder face.
- Similarly, a rail seat with a lower lateral stiffness results in a higher percentage of lateral load being restrained by adjacent rail seats or friction.
- Adjacent rail seat fastening systems can have considerable differences in lateral stiffness, and resulting magnitudes of lateral force under equivalent loading conditions.
- Increases in lateral stiffness of the fastening system as small as 32% can result in a 100% increase in the transfer of lateral load.
- The maximum measured lateral force when loaded directly over the corresponding LLED was just over 7,800 lbs (35 kN), 36% of the input lateral load. The minimum measured lateral force under the same loading conditions was just over 3,500 lbs (16 kN), 16% of the input lateral load.

Mechanistic design of future designs will benefit from these results by designing systems with optimum lateral load distribution between frictional interfaces and bearing surfaces. Additionally, the results from the experiments conducted with the LLED will be used to validate finite element modeling (FEM) work already underway at UIUC. Moreover, the results will be used for the mechanistic design of future fastening systems and their components to mitigate the performance problems currently seen on North American heavy-haul freight railroads.

FUTURE WORK

Future work will continue to focus on quantifying the lateral load path in concrete crosstie fastening systems. A more comprehensive laboratory and field instrumentation plan will be developed to further our understanding of different frictional interactions and the lateral load path. Future experimentation by UIUC researchers includes installing LLEDs on revenue service track in varying geometric conditions and in demanding traffic volumes. The first phase of field experimentation will be conducted using existing Safelok I fastening systems, but future research will involve applying the same technology and methodology to other types of fastening systems. Understanding how different designs perform under demanding conditions will assist researchers in altering the recommended practices for the benefit of the railroad industry as a whole.

Additionally, future research will focus on altering the insulator material to better understand how different insulator material properties affect the lateral stiffness of the system. Future research in this area will address the topic of material selection and ultimately enable manufacturers and railroads to specify the materials based on mechanistic design practices.

ACKNOWLEDGEMENTS

This project is sponsored by a grant from the Association of American Railroads (AAR) Technology Scanning Program with additional funding for field experimentation provided by the United States Department of Transportation (DOT) Federal Railroad Administration (FRA). The published material in this paper represents the position of the authors and not necessarily that of DOT. The authors would like to thank Dave Davis of AAR/TTCI; John Bosshart and Thomas Brueske of BNSF; Harold Harrison of H2 Visions, Inc.; Don Rhodes and Bill Rhodes of Instrumentation Services, Inc.; Tim Prunkard, Darold Marrow, and Don Marrow of the University of Illinois at Urbana-Champaign (UIUC); Jose Mediavilla of Amsted RPS; Jim Beyerl of CSX Transportation; Steve Ashmore and Chris Rewzyck of UPRR; and Bob Coats of Pandrol USA for their advice, guidance and contributions to this research. The authors would also like to acknowledge Daniel Kuchma, David Lange, Marcus Dersch, Thiago Bizarria, Christopher Rapp, Brandon Van Dyk, Sihang Wei, Justin Grasse, Kartik Manda, and Andrew Scheppe from UIUC for their work on this research. J. Riley Edwards has been supported in part by the grants to the UIUC Railroad Engineering Program from CN, CSX, Hanson Professional Service, Norfolk Southern, and the George Krambles Transportations Scholarship Fund.

REFERENCES

(1) Van Dyk, B. et al 2012. *International Concrete Crosstie and Fastening System Survey – Final Results*, University of Illinois at Urbana-Champaign, Results Released June 2012.
(2) Hay, W.W. *Railroad Engineering*, *2nd ed.*, John Wiley & Sons, Inc., New York City, New York, 1982, Ch. 23, pp. 471-473.
(3) *AREMA Manual for Railway Engineering*, American Railway Engineering and Maintenance-of-Way Association (AREMA), Landover, Maryland, 2012, v 1, ch. 30, parts 1 and 4.
(4) Stamatis, D, H. *Failure Mode and Effect Anaylsis: FMEA From Theory to Execution*.Vol.1. Milwaukee: ASQC Quality Press, 1995. 1-482. Print.
(5) Painter, P.C and M.M. Coleman. *Essentials of Polymer Science and Engineering,* DEStech Publications, Inc., Lancaster, PA.
(6) Van Dyk, B., J.R. Edwards, C.J. Ruppert, and C.P.L Barkan. 2013. Considerations for Mechanistic Design of Concrete Sleepers and Elastic Fastening Systems in North America. Proceedings of the 2013 International Heavy Haul Association Conference. New Delhi, India, (February 2013).
(7) Grasse, J. 2013. *Field Test Program of the Concrete Crosstie and Fastening System.* University of Illinois at Urbana-Champaign, Urbana, IL.
(8) Rapp, C.T., M. Dersch, J.R. Edwards, C.P.L. Barkan, B. Wilson, and J. Mediavilla. 2013. Measuring Concrete Crosstie Rail Seat Pressure Distribution with Matrix Based Tactile Surface Sensors. In: *Proceedings: Transportation Research Board Annual Meeting,* Washington D.C., United States, January 2013, pp. 2-3
(9) Rhodes, Don, Instrumentation Services, Inc. Personal interview, 19 March 2013.,
(10) Kerchof, B., H. Wu. Causes of Rail Cant and Controlling Cant Through Wheel/Rail Interface Management. In: *Proceedings of the 2012 Annual AREMA Conference,* Chicago, Illinois, September, 2012.
(11) Birmann, F. Track Parameters, Static and Dynamic. In: *Proceedings of Institution of Mechanical Engineers, Conference Proceedings Vol. Pt 3F,* June 1965, pp. 80-83.
(12) Chen, Z., M. Shin, B. Andrawes. 2013. Finite Element Modeling of the Fastening Systems and the Concrete Sleepers in North America. Proceedings of the 2013 International Heavy Haul Association Conference. New Delhi, India, (February 2013).
(13) Czichos, H. 1978. *Tribology: a systems approach to the science and technology of friction, lubrication and wear*, Elsevier North-Holland, Inc., New York, NY.